

Review of Inclusive Semileptonic B Decays and $B \rightarrow D^{(*)} \tau \nu$ at BaBar.

Concezio Bozzi^{*†}

INFN Sezione di Ferrara

E-mail: bozzi@fe.infn.it

A review of measurements of inclusive semileptonic decays of B mesons at the B Factories is presented. Results are reported for final states with and without charmed hadrons, and the resulting determinations of the CKM matrix elements $|V_{ub}|$ and $|V_{cb}|$ are shown. Inclusive measurements are internally consistent, however both $|V_{cb}|$ and $|V_{ub}|$ show a mild discrepancy with respect to determinations with exclusive semileptonic decays. A recent measurement of $B \rightarrow D^{(*)} \tau \nu$ decays at *BABAR* is also discussed. The results exceed the Standard Model expectation at the 3.4σ level. This excess cannot be explained by a charged Higgs boson in the type II two-Higgs-doublet model.

*The XIth International Conference on Heavy Quarks and Leptons,
June 11-15, 2012
Prague, Czech Republic*

^{*}Speaker.

[†]On behalf of the *BABAR* and Belle collaborations.

1. Introduction

Semileptonic decays of B mesons are sensitive to the magnitude of the CKM matrix elements $|V_{cb}|$ and $|V_{ub}|$, which complement the measurements of CP asymmetries, providing a stringent test of the CKM Unitarity Triangle. Moreover, these decays can be used also to determine Heavy Quark parameters (e.g. b and c -quark masses) and other quantities related to the dynamics of strong interactions. Measurements of semileptonic B decays at the B Factories offer several advantages with respect to other experimental environments. The final state consists only of particles resulting from the decay of the $B\bar{B}$ pair produced by the $\Upsilon(4S)$. The $B\bar{B}$ cross-section at the $\Upsilon(4S)$ is about 1.05 nb , with an acceptable (0.25) ratio to continuum $e^+e^- \rightarrow q\bar{q}$ background. The high integrated luminosities collected at the B Factories (roughly 1.2 ab^{-1} in total) and the large $B \rightarrow X\ell\bar{\nu}$ branching fraction results in inclusive samples of the order of several million events. The reconstruction of semileptonic decays is based on the excellent charged lepton identification of B Factories experiments, and on accurate measurements of the hadronic system accompanying the lepton pair. The neutrino is indirectly reconstructed by measuring the momentum and energy of all particles in an event and comparing the resulting four-vector with the known initial state energy-momentum. To study inclusive semileptonic decays, it is important to correctly assign particles to the hadronic system produced in the semileptonic decay. This is a difficult task at the $\Upsilon(4S)$, since the two B mesons are produced at rest and particles from the two decays are isotropically distributed and therefore tend to overlap. For this reason, a technique has been developed by which one of the two B mesons (B_{reco}) in the event is fully reconstructed in an hadronic decay mode and semileptonic decays are searched for in the other (B_{recoil}). All particles not belonging to the B_{reco} and not identified with a lepton are associated to the hadronic system X , whose kinematic properties are therefore completely determined. This *hadronic tag* method also gives an improved neutrino reconstruction and a reduction of combinatorial backgrounds. However, the resulting reconstruction efficiencies are only of a few permille (0.3-0.6%). The resulting inclusive samples collected at the B Factories are therefore of the order of one hundred thousand and one thousand for $\bar{B} \rightarrow X_c\ell\bar{\nu}$ and $B \rightarrow X_u\ell\bar{\nu}$ decays, respectively.

From the theoretical point of view, the quark-level decay rate is given by

$$\Gamma(b \rightarrow q\ell\nu) = \frac{G_F^2 m_b^5}{192\pi^3} |V_{qb}|^2 (1 + A_{ew}) \quad (1.1)$$

where A_{ew} is due to electroweak corrections and $q = c, u$. At the hadron level, one needs to take into account effects due to the strong interactions between the quarks. Due to the large mass of the b quark, an Operator Product Expansion (OPE) approach can be used to factorize the contributions due long- and short-distance dynamics. The former, non-perturbative contributions, are given by matrix elements of local operators, while the latter enter as coefficients in front of these operators, and can be calculated in perturbation theory. This results in a double-series expansion in powers of α_s and $1/m_b$ [1, 2]. The total decay rate can be schematically written as [3]

$$\Gamma(B \rightarrow X_q\ell\nu) = \frac{G_F^2 m_b^5(\mu)}{192\pi^3} |V_{qb}|^2 (1 + A_{ew}) \cdot \left\{ \sum_i (\alpha_s(\mu))^i [z_0^{(i)}(r) + \frac{\mu_\pi^2}{m_b^2} z_2^{(i)}(r) + \frac{\mu_G^2}{m_b^2} y_2^{(i)}(r) + \frac{\rho_D^3}{m_b^3} z_3^{(i)}(r) + \frac{\rho_{LS}^3}{m_b^3} y_3^{(i)}(r) + \dots] \right\}$$

where $r = m_q/m_b$, y_i and z_i are known functions which appear in the perturbative expansion of the different orders of the heavy mass expansion, and μ is the renormalization scale. Conceptually similar expressions can be calculated for differential rates. Non-perturbative inputs, e.g. μ_π^2 , μ_G^2 , ρ_D^3 and ρ_{LS}^3 up to the third order in $1/m_b$, are not calculable from first principles, but they enter in a well-defined way in experimentally accessible spectral moments, e.g. the *lepton energy-hadronic mass* moments:

$$\langle E_\ell^n M_X^{2n} \rangle = \frac{1}{\Gamma_0} \int_{E_{min}}^{E_{max}} dE_\ell \int dM_X^2 \frac{d\Gamma(\mu_\pi^2, \mu_G^2, \rho_D^3, \rho_{LS}^3, \dots)}{dE_\ell dM_X^2} E_\ell^n M_X^{2n} \quad (1.2)$$

A *global fit* to moments allows to determine $|V_{qb}|$ and non-perturbative inputs, as well as the masses of the beauty and charm quarks.

2. Inclusive $\bar{B} \rightarrow X_c \ell \bar{\nu}$ decays and the determination of $|V_{cb}|$

Following the path outlined at the end of the last section, a vast experimental program has been carried out in order to measure distributions of relevant quantities in inclusive semileptonic decays and several moments for each of them. While observables such as the lepton energy are conceptually easy to measure, the energy and invariant mass of the hadronic system are best determined in events with an hadronic tag. Background discrimination is based on the inferred neutrino momentum and squared missing mass. Proper calibration of the hadronic observables is needed and an unfolding procedure is necessary to deconvolute detector effects and measure quantities which can be directly related to the spectra and moments predicted by theory. Measurements have been performed at the B Factories [4, 5, 6, 7, 8, 9, 10], but also at CLEO [11, 12], CDF [13] and DELPHI [14]. Many moments are extracted from a single distribution, therefore large correlations need to be taken into account. Moreover, moments are extracted by integrating data above cuts on the lepton energy E_{min} . The leading experimental systematic uncertainties are due to detector modeling and to the knowledge of B and D decays. The CKM matrix element $|V_{cb}|$, the mass of the charm and beauty quarks and other hadronic parameters are determined from a fit to theory predictions, which are accurate up to second-order terms in α_s and third order terms in $1/m_b$. Theoretical calculations are performed by using either the kinetic [2, 15, 16] or 1S renormalization schemes [17]. Although effective in determining $|V_{cb}|$, the moments of $\bar{B} \rightarrow X_c \ell \bar{\nu}$ decays are not sufficient to constrain the b quark mass precisely, which is important for the determination of $|V_{ub}|$ with inclusive decays. This limitation can be overcome by including the photon energy moments in inclusive $B \rightarrow X_s \gamma$ decays [18] into the fit, or by applying a precise constraint on the c quark mass. For the latter, a quite conservative determination [19] of $m_c(3GeV) = 0.998 \pm 0.029$ GeV in the \overline{MS} scheme is used. The global fit in the kinetic scheme, using the charm quark mass constraint, gives

$$|V_{cb}| = (41.88 \pm 0.44_{fit} \pm 0.59_{theory}) \times 10^{-3}.$$

This result is consistent with the fit using the $B \rightarrow X_s \gamma$ constraint (see table 1). While the value of $|V_{cb}|$ is barely affected, the value of the b quark mass decreases by about 15 MeV and its uncertainty decreases from 32 to 23 MeV. Similar results are obtained in the 1S scheme. In summary, $|V_{cb}|$ is determined at the 2% level and its determination is nearly independent of the renormalization

scheme and constraints imposed. The value of $|V_{cb}|$ obtained with inclusive decays is about 2σ higher than the one measured with exclusive semileptonic decays [20].

Table 1: Global fit results in the kinetic scheme for different constraints. Refer to the text for more details.

Constraint	$ V_{cb} [10^{-3}]$	$m_b^{\text{kin}} [\text{GeV}]$	$\mu_\pi^2 [\text{GeV}^2]$	$\chi^2/\text{d.o.f.}$
$B \rightarrow X_s \gamma$	$41.94 \pm 0.43_{\text{fit}} \pm 0.59_{\text{th}}$	4.574 ± 0.032	0.459 ± 0.037	$27.0/(66 - 7)$
$m_c^{\overline{\text{MS}}}(3 \text{ GeV})$	$41.88 \pm 0.44_{\text{fit}} \pm 0.59_{\text{th}}$	4.560 ± 0.023	0.453 ± 0.036	$33.4/(55 - 7)$

3. Inclusive $B \rightarrow X_u \ell \bar{\nu}$ decays

Due to the much more abundant $\bar{B} \rightarrow X_c \ell \bar{\nu}$ background, the study of inclusive charmless semileptonic decays is experimentally challenging. Kinematical cuts are required to suppress backgrounds. Therefore only partial branching fraction can be measured, and the extrapolation to the full phase space must rely on theoretical predictions. Also, relevant variables to discriminate signal over background, such as the invariant mass of the hadronic system m_X and the squared invariant mass of the lepton pair q^2 , can be accessed only in hadronically tagged events.

From the theoretical point of view, cutting on kinematic variables may be problematic, since in limited phase space regions OPE breaks down and a shape function, not calculable from first principles, is needed to resum non perturbative processes [21, 22, 23]. It is in principle possible to measure the leading shape function in radiative $B \rightarrow X_s \gamma$ decays, and apply the results to the calculation of $B \rightarrow X_u \ell \bar{\nu}$ partial decay rates [24, 25]. However, subleading shape functions appear at each order in $1/m_b$, which are different in semileptonic and radiative decays, thus limiting the ultimate theoretical accuracy. The most promising approach is to extend measurements of $B \rightarrow X_u \ell \bar{\nu}$ partial rates in regions where $\bar{B} \rightarrow X_c \ell \bar{\nu}$ is allowed and the theoretical treatment simplified. Precise knowledge of the $\bar{B} \rightarrow X_c \ell \bar{\nu}$ background is in this case the factor limiting the $|V_{ub}|$ accuracy. Measurements in as many phase space regions as possible is in any case important to check the theoretical calculations predicting the corresponding partial rates and give constraints on the shape function. Theoretical calculations can be roughly grouped in two classes, inspired respectively by OPE (BLNP [26, 27, 28, 29], GGOU [30]) and resummed perturbation theory (DGE [31], ADFR [32]).

The most precise measurements are performed by *BABAR* and Belle on a region defined by $p_\ell^* > 1 \text{ GeV}$. Signal and background discrimination is achieved by fitting the m_X and q^2 spectra. While *BABAR* performs a cut-based analysis, Belle relies on a multivariate analysis. In both cases, measurements are performed in the system recoiling against a fully reconstructed B decay. Figure 1 shows the distributions obtained by *BABAR*. In these inclusive measurements, the systematic uncertainties are dominated by signal modeling, and the total uncertainties on the partial branching fractions is of the order of 12%.

Measurements of partial branching fractions for $B \rightarrow X_u \ell \bar{\nu}$ decays, together with the corresponding accepted region, are given in Table 2.

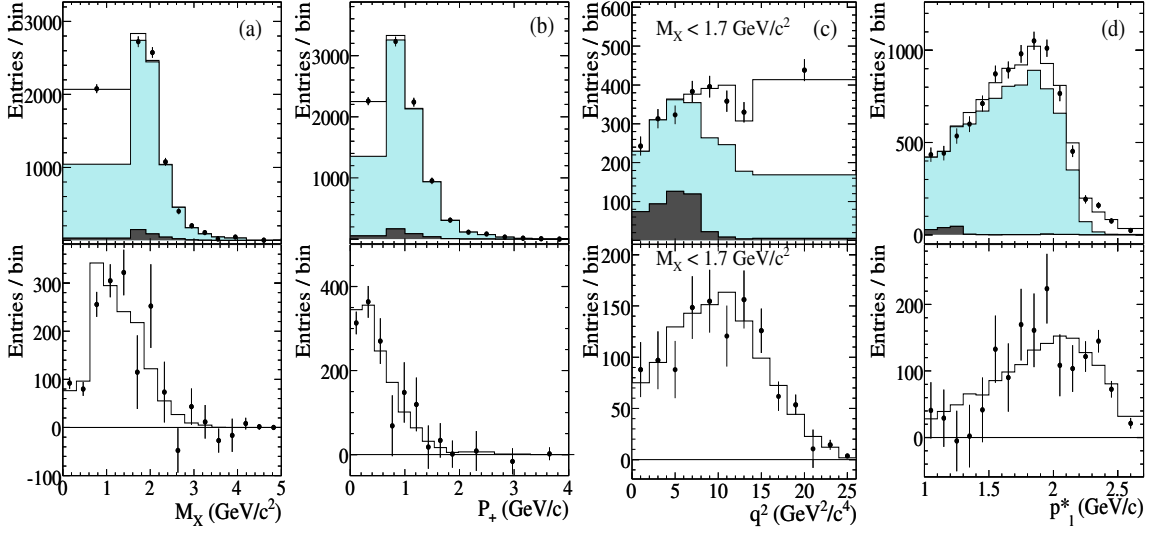


Figure 1: Upper row: measured m_X (a), P_+ (b), q^2 with $m_X < 1.7 \text{ GeV}/c^2$ (c) and p_ℓ^* spectra (d) (data points). The white and black histogram represent $B \rightarrow X_u \ell \bar{\nu}$ decays generated respectively inside and outside the selected kinematic region. Light-shaded histograms represent $\bar{B} \rightarrow X_c \ell \bar{\nu}$ and other backgrounds. Lower row: Background-subtracted spectra, not efficiency-corrected. *BABAR* data.

Table 2: Summary of inclusive determinations of partial branching fractions for $B \rightarrow X_u \ell \bar{\nu}$ decays. The errors quoted on $\Delta\mathcal{B}$ correspond to statistical and systematic uncertainties. The s_h^{\max} variable is described in Refs. [33, 34].

Measurement	Accepted region	$\Delta\mathcal{B}[10^{-4}]$
CLEO [35]	$E_e > 2.1 \text{ GeV}$	$3.3 \pm 0.2 \pm 0.7$
<i>BABAR</i> [34]	$E_e > 2.0 \text{ GeV}, s_h^{\max} < 3.5 \text{ GeV}^2$	$4.4 \pm 0.4 \pm 0.4$
<i>BABAR</i> [36]	$E_e > 2.0 \text{ GeV}$	$5.7 \pm 0.4 \pm 0.5$
BELLE [37]	$E_e > 1.9 \text{ GeV}$	$8.5 \pm 0.4 \pm 1.5$
<i>BABAR</i> [38]	$M_X < 1.7 \text{ GeV}/c^2, q^2 > 8 \text{ GeV}^2/c^2$	$6.8 \pm 0.6 \pm 0.4$
BELLE [39]	$M_X < 1.7 \text{ GeV}/c^2, q^2 > 8 \text{ GeV}^2/c^2$	$7.4 \pm 0.9 \pm 1.3$
BELLE [40]	$M_X < 1.7 \text{ GeV}/c^2, q^2 > 8 \text{ GeV}^2/c^2$	$8.4 \pm 0.8 \pm 1.0$
<i>BABAR</i> [38]	$P_+ < 0.66 \text{ GeV}$	$9.8 \pm 0.9 \pm 0.8$
<i>BABAR</i> [38]	$M_X < 1.7 \text{ GeV}/c^2$	$11.5 \pm 1.0 \pm 0.8$
<i>BABAR</i> [38]	$M_X < 1.55 \text{ GeV}/c^2$	$10.8 \pm 0.8 \pm 0.6$
BELLE [41]	$p_\ell^* > 1 \text{ GeV}/c$	$19.6 \pm 1.7 \pm 1.6$
<i>BABAR</i> [38]	(M_X, q^2) fit, $p_\ell^* > 1 \text{ GeV}/c$	$18.0 \pm 1.3 \pm 1.5$
<i>BABAR</i> [38]	$p_\ell^* > 1.3 \text{ GeV}/c$	$15.3 \pm 1.3 \pm 1.4$

4. $|V_{ub}|$ determination

The magnitude of $|V_{ub}|$ is determined from the partial branching fraction measurements shown above as

$$|V_{ub}| = \sqrt{\frac{\Delta\mathcal{B}(B \rightarrow X_u \ell \bar{\nu})}{\tau_B \Delta\Gamma_{\text{theory}}}}, \quad (4.1)$$

where $\Delta\Gamma_{\text{theory}}$, the theoretically predicted $B \rightarrow X_u \ell \bar{\nu}$ rate for the selected phase space region, is determined by the four calculations discussed in the previous section (BLNP, DGE, GGOU, ADFR), and τ_B is the B meson lifetime. Table 3 shows the results, as well as the resulting averages. A fifth calculation (BLL [24]), which gives an HQET-based prescription for phase space regions defined by combined cuts on m_X, q^2 , is also shown.

The total uncertainty on the resulting $|V_{ub}|$ averages is of the order of 6% for all methods but BLL. The consistency between measurements in different phase space regions is good. The most inclusive measurements ($p_\ell^* > 1\text{GeV}$) give very consistent $|V_{ub}|$ values for all theoretical calculations, while the spread between the calculations increases in restricted regions of phase space (e.g. in the endpoint analyses).

Table 3: Summary of input parameters used by the different theory calculations, corresponding inclusive determinations of $|V_{ub}|$ and their average. The errors quoted on $|V_{ub}|$ correspond to experimental and theoretical uncertainties, respectively.

	BLNP	DGE	GGOU	ADFR	BLL
Input parameters					
scheme	SF	\overline{MS}	kinetic	\overline{MS}	1S
m_b (GeV)	4.588 ± 0.025	4.194 ± 0.043	4.560 ± 0.023	4.194 ± 0.043	4.704 ± 0.029
μ_π^2 (GeV ²)	$0.189^{+0.046}_{-0.057}$	-	0.453 ± 0.036	-	-
Ref.	$ V_{ub} $ values				
E_e [35]	$4.19 \pm 0.49^{+0.26}_{-0.34}$	$3.82 \pm 0.45^{+0.23}_{-0.26}$	$3.93 \pm 0.46^{+0.22}_{-0.29}$	$3.43 \pm 0.40^{+0.16}_{-0.17}$	-
M_X, q^2 [39]	$4.46 \pm 0.47^{+0.25}_{-0.27}$	$4.40 \pm 0.46^{+0.19}_{-0.20}$	$4.37 \pm 0.46^{+0.23}_{-0.26}$	$3.89 \pm 0.41^{+0.17}_{-0.18}$	$4.68 \pm 0.49^{+0.30}_{-0.30}$
E_e [37]	$4.88 \pm 0.45^{+0.24}_{-0.27}$	$4.79 \pm 0.44^{+0.21}_{-0.24}$	$4.75 \pm 0.44^{+0.17}_{-0.22}$	$4.48 \pm 0.42^{+0.20}_{-0.20}$	-
E_e [36]	$4.48 \pm 0.25^{+0.27}_{-0.28}$	$4.28 \pm 0.24^{+0.22}_{-0.24}$	$4.29 \pm 0.24^{+0.18}_{-0.24}$	$3.94 \pm 0.22^{+0.19}_{-0.20}$	-
E_e, s_h^{max} [34]	$4.66 \pm 0.31^{+0.31}_{-0.36}$	$4.32 \pm 0.29^{+0.24}_{-0.29}$	-	$3.82 \pm 0.26^{+0.17}_{-0.18}$	-
p_ℓ^* [41]	$4.47 \pm 0.27^{+0.19}_{-0.21}$	$4.60 \pm 0.27^{+0.11}_{-0.13}$	$4.54 \pm 0.27^{+0.10}_{-0.11}$	$4.48 \pm 0.30^{+0.19}_{-0.19}$	-
$M_X < 1.55\text{GeV}$ [38]	$4.17 \pm 0.19^{+0.24}_{-0.24}$	$4.40 \pm 0.20^{+0.24}_{-0.19}$	$4.08 \pm 0.19^{+0.20}_{-0.21}$	$3.81 \pm 0.18^{+0.18}_{-0.20}$	-
$M_X < 1.7\text{GeV}$ [38]	$3.97 \pm 0.22^{+0.20}_{-0.20}$	$4.16 \pm 0.23^{+0.26}_{-0.22}$	$3.94 \pm 0.22^{+0.16}_{-0.17}$	$3.73 \pm 0.21^{+0.17}_{-0.18}$	-
M_X, q^2 [38]	$4.25 \pm 0.23^{+0.23}_{-0.25}$	$4.19 \pm 0.22^{+0.18}_{-0.19}$	$4.17 \pm 0.22^{+0.22}_{-0.25}$	$3.74 \pm 0.20^{+0.16}_{-0.17}$	$4.50 \pm 0.24^{+0.29}_{-0.29}$
P_+ [38]	$4.02 \pm 0.25^{+0.24}_{-0.23}$	$4.10 \pm 0.25^{+0.37}_{-0.28}$	$3.75 \pm 0.23^{+0.30}_{-0.32}$	$3.56 \pm 0.22^{+0.18}_{-0.19}$	-
$P^* > 1\text{GeV}$ [38]	$4.28 \pm 0.24^{+0.18}_{-0.20}$	$4.40 \pm 0.24^{+0.12}_{-0.13}$	$4.35 \pm 0.24^{+0.09}_{-0.10}$	$4.29 \pm 0.24^{+0.18}_{-0.19}$	-
$P^* > 1.3\text{GeV}$ [38]	$4.29 \pm 0.27^{+0.19}_{-0.20}$	$4.39 \pm 0.27^{+0.15}_{-0.14}$	$4.33 \pm 0.27^{+0.10}_{-0.11}$	$4.27 \pm 0.26^{+0.18}_{-0.19}$	-
M_X, q^2 [40]	-	-	-	-	$5.01 \pm 0.39^{+0.32}_{-0.32}$
Average	$4.40 \pm 0.15^{+0.19}_{-0.21}$	$4.45 \pm 0.15^{+0.15}_{-0.16}$	$4.39 \pm 0.15^{+0.12}_{-0.14}$	$4.03 \pm 0.13^{+0.18}_{-0.12}$	$4.62 \pm 0.20^{+0.29}_{-0.29}$

The arithmetic average of the BLNP, DGE, GGOU and ADFR averages gives

$$|V_{ub}| = (4.33 \pm 0.24_{\text{exp}} \pm 0.15_{\text{theo}}) 10^{-3},$$

which is about 2.5σ higher than the $|V_{ub}|$ determination with exclusive charmless semileptonic decays [20].

5. Evidence for an excess of $B \rightarrow D^{(*)} \tau \bar{\nu}$ decays at BABAR

Semileptonic decays with a τ lepton in the final state are sensitive to processes involving

non-Standard Model particles, and particularly to charged Higgs bosons which would appear as propagator in the Feynman diagram. The ratios $R(D^{(*)})$ of decays with taus and lighter leptons in the final state is predicted at the 5-10% level in the Standard model [42, 43]:

$$R(D) = \frac{\mathcal{B}(B \rightarrow D \tau \bar{\nu})}{\mathcal{B}(\bar{B} \rightarrow D \ell \bar{\nu})} = 0.297 \pm 0.017$$

$$R(D^*) = \frac{\mathcal{B}(B \rightarrow D^* \tau \bar{\nu})}{\mathcal{B}(\bar{B} \rightarrow D^* \ell \bar{\nu})} = 0.252 \pm 0.003$$

Both $B \rightarrow D \tau \bar{\nu}$ and $B \rightarrow D^* \tau \bar{\nu}$ have been previously established with 3.8σ and 8.1σ significances [44, 45, 46, 47], but the experimental sensitivity was not sufficient to give meaningful constraints on new physics. A new analysis of BABAR data has been performed [48], following the same philosophy of the previous one, but using the entire dataset ($\mathcal{L} = 426 fb^{-1}$) and improving the reconstruction of the hadronic B decay against which signal is searched for. Improvements in particle identification and background rejection were also achieved.

Four samples are defined, according to the reconstructed D meson (D^0, D^+, D^{*0}, D^{*+}), and the tau meson is reconstructed in leptonic final states. In this way, signal samples have the same detectable particles as *normalization samples*, i.e. decays into lighter leptons. A poorly known remaining background is due decays into P-wave charmed mesons (D^{**}). These are studied with four control samples (one for each signal sample), selected by adding a neutral pion to the decay chain. A simultaneous fit is performed to the distribution of the lepton momentum in the B rest frame, p_ℓ^* , and the square of the missing mass. The fit gives the yields for signal, normalization and control samples simultaneously for the four different charm mesons involved in the final state. The other background yields and shapes are determined from simulations, after data-driven corrections have been applied. These residual backgrounds include: charge cross-feed, giving a contamination from B^+ decays, and combinatorial background from $B\bar{B}$ and continuum events. Isospin constraints can be also imposed in order to get a combined measurement for B^+ and B^0 decays. The results of the fit are shown in Figure 2. The signal yields, signal significance and measured values of $R(D)$ and $R(D^*)$ are reported in table 4. Systematic uncertainties are dominated by the assumptions made on the D^{**} background, the statistical accuracy of the simulation and the knowledge of continuum and $B\bar{B}$ backgrounds. The correlation between $R(D)$ and $R(D^*)$ is -27%.

Table 4: Results of the isospin-unconstrained (top four rows) and isospin-constrained fits (last two rows). The columns show the signal and normalization yields, $R^{(*)}$, branching fractions, and Σ_{stat} and Σ_{tot} , the statistical and total significances.

Decay	N_{sig}	N_{norm}	$R^{(*)}$	$\mathcal{B}(B \rightarrow D^{(*)} \tau \nu)$ (%)	Σ_{stat}	Σ_{tot}
$B^- \rightarrow D^0 \tau^- \bar{\nu}_\tau$	314 ± 60	1995 ± 55	$0.429 \pm 0.082 \pm 0.052$	$0.99 \pm 0.19 \pm 0.13$	5.5	4.7
$B^- \rightarrow D^{*0} \tau^- \bar{\nu}_\tau$	639 ± 62	8766 ± 104	$0.322 \pm 0.032 \pm 0.022$	$1.71 \pm 0.17 \pm 0.13$	11.3	9.4
$\bar{B}^0 \rightarrow D^+ \tau^- \bar{\nu}_\tau$	177 ± 31	986 ± 35	$0.469 \pm 0.084 \pm 0.053$	$1.01 \pm 0.18 \pm 0.12$	6.1	5.2
$\bar{B}^0 \rightarrow D^{*+} \tau^- \bar{\nu}_\tau$	245 ± 27	3186 ± 61	$0.355 \pm 0.039 \pm 0.021$	$1.74 \pm 0.19 \pm 0.12$	11.6	10.4
$\bar{B} \rightarrow D \tau^- \bar{\nu}_\tau$	489 ± 63	2981 ± 65	$0.440 \pm 0.058 \pm 0.042$	$1.02 \pm 0.13 \pm 0.11$	8.4	6.8
$\bar{B} \rightarrow D^* \tau^- \bar{\nu}_\tau$	888 ± 63	11953 ± 122	$0.332 \pm 0.024 \pm 0.018$	$1.76 \pm 0.13 \pm 0.12$	16.4	13.2

6. Implications on the Standard Model and new physics

The two measurements of $R(D)$ and $R(D^*)$ exceed the Standard Model prediction by 2.0σ and

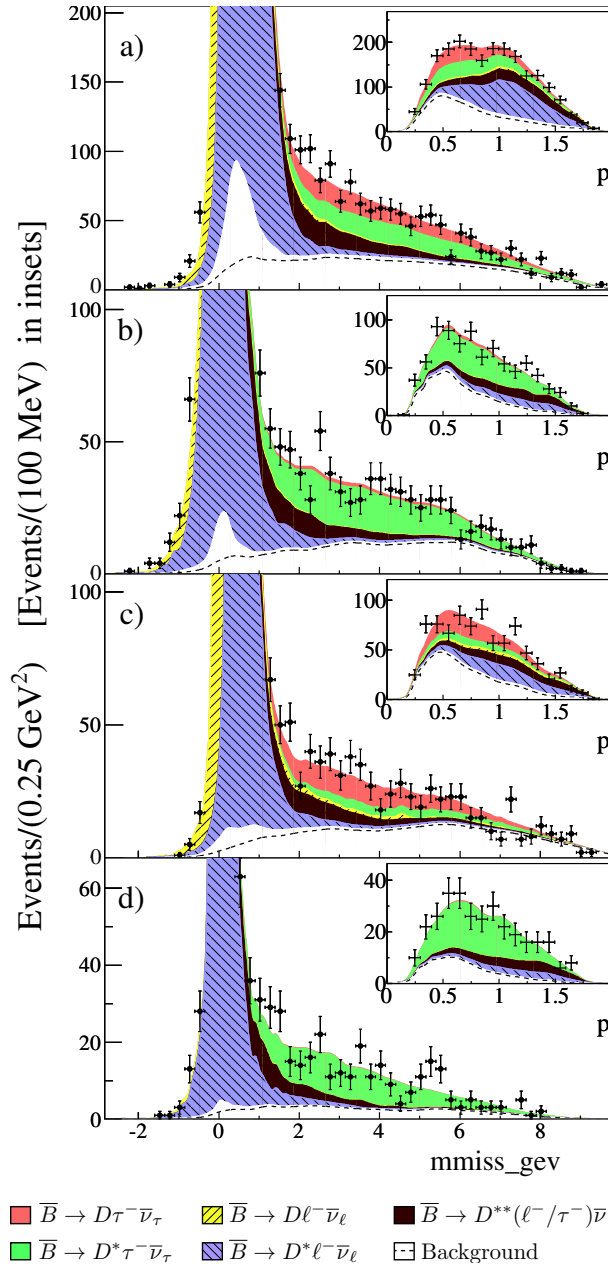


Figure 2: Data and the fit projections in the m_{miss}^2 variable for the four $D^{(*)}\ell$ samples. The insets show the p_ℓ^* projections for $m_{miss}^2 > 1\text{GeV}^2$, which excludes most of the normalization modes. In the background component, the region above the dashed line corresponds to charge cross-feed, and the region below corresponds to continuum and $B\bar{B}$.

2.7σ , respectively. Their combination, including their correlation, gives a p -value of 6.9×10^{-4} . Therefore, the possibility of both measurements to agree with the Standard Model is excluded at the 3.4σ level.

The effect that a charged Higgs boson, in a two-Higgs-doublet model of type II [49, 50], would have on the measurements is evaluated by reweighting the relevant matrix element in the simulation

according to 20 different values of $\tan \beta / m_{H^+}$, where $\tan \beta = v_2 / v_1$ is the ratio of the expectation values, and repeating the analysis. The regions allowed by the $R(D)$ and $R(D^*)$ measurements are $\tan \beta / m_{H^+} = 0.44 \pm 0.02$ and $\tan \beta / m_{H^+} = 0.75 \pm 0.04$, respectively. Their combination excludes the full parameter space of this model with 99.8% probability, in the region $m_{H^+} > 10 \text{ GeV}$.

7. Conclusion

After ten years of efforts, the determination of $|V_{cb}|$, $|V_{ub}|$ and the b quark mass with inclusive semileptonic decays of B mesons has improved substantially both from the theoretical and the experimental point of view, resulting in accuracies at the (few) percent level. Long-standing 2-3 σ tensions between inclusive and exclusive determinations and CKM fits are still present in data, signaling either that the current understanding of QCD is still above the percent level or perhaps that there might be new physics effects in $b \rightarrow u$ transitions.

Finally, a significant excess of events in $B \rightarrow D \tau \bar{\nu}$ and $B \rightarrow D^* \tau \bar{\nu}$ decays, marginally compatible with the SM and clearly disfavoring a 2-Higgs Doublet Model of type II, has been observed by BABAR. This prompts for further investigations from current experiments and future facilities.

References

- [1] A. V. Manohar and M. B. Wise, *Phys.Rev.* **D49**, 1310–1329, (1994).
- [2] D. Benson, I. I. Bigi, T. Mannel, and N. Uraltsev, *Nucl. Phys.* **B665**, 367–401, (2003).
- [3] I. I. Bigi, B. Blok, M. A. Shifman, and A. I. Vainshtein, *Phys.Lett.* **B323**, 408–416, (1994).
- [4] B. Aubert *et al.*, (BABAR collaboration), *Phys. Rev.* **D72**, 052004, (2005).
- [5] B. Aubert *et al.*, (BaBar collaboration), *Phys.Rev.Lett.* **97**, 171803, (2006).
- [6] B. Aubert *et al.*, (BABAR collaboration), *Phys. Rev.* **D81**, 032003, (2010).
- [7] B. Aubert *et al.*, (BABAR collaboration), *Phys. Rev.* **D69**, 111104, (2004).
- [8] C. Schwanda *et al.*, (Belle collaboration), *Phys. Rev.* **D75**, 032005, (2007).
- [9] A. Limosani *et al.*, (Belle collaboration), *Phys. Rev. Lett.* **103**, 241801, (2009).
- [10] P. Urquijo *et al.*, (Belle collaboration), *Phys. Rev.* **D75**, 032001, (2007).
- [11] S. Chen *et al.*, (CLEO collaboration), *Phys.Rev.Lett.* **87**, 251807, (2001).
- [12] S. E. Csorna *et al.*, (CLEO collaboration), *Phys. Rev.* **D70**, 032002, (2004).
- [13] D. E. Acosta *et al.*, (CDF collaboration), *Phys. Rev.* **D71**, 051103, (2005).
- [14] J. Abdallah *et al.*, (DELPHI collaboration), *Eur. Phys. J.* **C45**, 35–59, (2006).
- [15] P. Gambino and N. Uraltsev, *Eur. Phys. J.* **C34**, 181–189, (2004).
- [16] P. Gambino, *JHEP* **1109**, 055, (2011).
- [17] C. W. Bauer, Z. Ligeti, M. Luke, A. V. Manohar, and M. Trott, *Phys. Rev.* **D70**, 094017, (2004).
- [18] D. Benson, I. I. Bigi, and N. Uraltsev, *Nucl. Phys.* **B710**, 371–401, (2005).
- [19] B. Dehnadi, A. H. Hoang, V. Mateu, and S. M. Zebarjad, (2011).

- [20] Y. Amhis *et al.*, (Heavy Flavor Averaging Group collaboration), (2012), [arXiv:1207.1158 \[hep-ex\]](#).
- [21] M. Neubert, *Phys.Rev.* **D49**, 4623–4633, (1994).
- [22] M. Neubert, *Phys.Rev.* **D49**, 3392–3398, (1994).
- [23] I. I. Bigi, M. A. Shifman, N. Uraltsev, and A. Vainshtein, *Int.J.Mod.Phys.* **A9**, 2467–2504, (1994).
- [24] C. W. Bauer, M. Luke, and T. Mannel, *Phys.Lett.* **B543**, 261–268, (2002).
- [25] T. Mannel and S. Recksiegel, *Phys.Rev.* **D60**, 114040, (1999).
- [26] B. O. Lange, M. Neubert, and G. Paz, *Phys. Rev.* **D72**, 073006, (2005).
- [27] S. W. Bosch, B. O. Lange, M. Neubert, and G. Paz, *Nucl. Phys.* **B699**, 335–386, (2004).
- [28] S. W. Bosch, M. Neubert, and G. Paz, *JHEP* **11**, 073, (2004).
- [29] M. Neubert, *Eur. Phys. J.* **C44**, 205–209, (2005).
- [30] P. Gambino, P. Giordano, G. Ossola, and N. Uraltsev, *JHEP* **10**, 058, (2007).
- [31] J. R. Andersen and E. Gardi, *JHEP* **01**, 097, (2006).
- [32] U. Aglietti, F. Di Lodovico, G. Ferrera, and G. Ricciardi, *Eur. Phys. J.* **C59**, 831–840, (2009).
- [33] R. V. Kowalewski and S. Menke, *Phys. Lett.* **B541**, 29–34, (2002).
- [34] B. Aubert *et al.*, (BABAR collaboration), *Phys. Rev. Lett.* **95**, 111801, (2005).
- [35] A. Bornheim *et al.*, (CLEO collaboration), *Phys. Rev. Lett.* **88**, 231803, (2002).
- [36] B. Aubert *et al.*, (BABAR collaboration), *Phys. Rev.* **D73**, 012006, (2006).
- [37] A. Limosani *et al.*, (Belle collaboration), *Phys. Lett.* **B621**, 28–40, (2005).
- [38] J. Lees, (Babar collaboration), (2011), [arXiv:1112.0702 \[hep-ex\]](#).
- [39] H. Kakuno *et al.*, (Belle collaboration), *Phys. Rev. Lett.* **92**, 101801, (2004).
- [40] I. Bizjak *et al.*, (Belle collaboration), *Phys. Rev. Lett.* **95**, 241801, (2005).
- [41] P. Urquijo *et al.*, (Belle collaboration), *Phys. Rev. Lett.* **104**, 021801, (2010).
- [42] J. F. Kamenik and F. Mescia, *Phys.Rev.* **D78**, 014003, (2008).
- [43] S. Fajfer, J. F. Kamenik, and I. Nisandzic, *Phys.Rev.* **D85**, 094025, (2012).
- [44] A. Matyja *et al.*, (Belle collaboration) *Phys. Rev. Lett.* **99**, 191807, (Nov, 2007).
- [45] B. Aubert *et al.*, (BABAR collaboration), *Phys.Rev.Lett.* **100**, 021801, (2008).
- [46] I. Adachi *et al.*, (Belle collaboration), (2009), [arXiv:0910.4301 \[hep-ex\]](#).
- [47] A. Bozek *et al.*, (Belle collaboration), *Phys.Rev.* **D82**, 072005, (2010).
- [48] J. Lees *et al.*, (BaBar collaboration), (2012), [arXiv:1205.5442 \[hep-ex\]](#).
- [49] M. Tanaka and R. Watanabe, *Phys. Rev. D* **82**, 034027, (2010).
- [50] V. D. Barger, J. Hewett, and R. Phillips, *Phys. Rev. D* **41**, 3421–3441, (1990).